Available online at www.sciencedirect.com

SciVerse ScienceDirect

journal homepage: www.elsevier.com/locate/he

The influence of carbon based supports and the role of synthesis procedures on the formation of platinum and platinum-ruthenium clusters and nanoparticles for the development of highly active fuel cell catalysts

Qi-Ling Naidoo [a], Sivapregasen Naidoo [a], Leslie Petrik [a], Alexander Nechaev [a], Patrick Ndungu [b,*]

[a] Environmental and Nanosciences Research Group, Department of Chemistry, University of the Western Cape, Bellville, South Africa
[b] School of Chemistry, University of KwaZulu-Natal, Westville Campus, Private Bag X54001, Durban 4000, South Africa

ARTICLE INFO

Article history:
Received 22 November 2011
Received in revised form
5 March 2012
Accepted 11 March 2012
Available online 10 April 2012

Keywords:
Platinum group metals
Metal-organic chemical vapour deposition
Electrocatalysts
Carbon nanotubes
Direct methanol fuel cell

ABSTRACT

A simple but effective solvent free method for the synthesis of platinum group metal nanoparticles on carbon nanotubes is presented. The initial work directly compares a typical wet chemical method and an organo-metallic chemical vapour deposition (OMCVD) technique for the production of 10 wt% Platinum on activated carbon and carbon nanotubes. The results obtained clearly showed that the wet chemical method produced materials with poorer physical-chemical characteristics and electrocatalytic activity. Also, carbon nanotubes were shown to be a more effective support regardless of the method of synthesis. Subsequent experimental work focused on the use of carbon nanotubes as a support, and the metal-organic chemical vapour deposition method as the synthesis technique. The method was successfully used to produce multiple samples with loadings of 20, 40 and 60 wt% Pt/CNT and a 40 wt% PtRu/CNT. HRTEM studies revealed stabilized clusters of platinum within CNT defects on samples synthesized using the OMCVD technique. The particle size distribution was relatively narrow, and the electrocatalytic activity was comparable or better than the benchmark Johnson Mathey 40 wt% Pt/C or 40 wt% PtRu/C.

Copyright © 2012, Hydrogen Energy Publications, LLC. Published by Elsevier Ltd. All rights reserved.

1. Introduction

Fuel cells are electrochemical energy conversion devices that are quiet, energy efficient, and can be very environmentally friendly. The key catalysts that enable the electrochemical process in a membrane type fuel cell are platinum based. There are several examples of non-platinum catalysts in fuel cells [1,2]; however platinum remains the favoured catalyst due to stability, activity, and excellent kinetics [3–6]. When utilizing hydrogen and oxygen, fuel cells are a clean source of energy with the only emissions being heat and water vapour. Use of hydrocarbon fuels as energy source for fuel cells can be considered as less desirable due to the production of carbon dioxide; however, the efficiency of the fuel cell systems and little or no sulphur and nitrogen oxides may outweigh some of these perceived disadvantages, especially when compared to internal combustion engines. In addition, small hydrocarbon feed molecules like methanol can be a very promising

* *Corresponding author*. Tel.: +27 (0) 31 260 3097; fax: +27 (0) 31 260 3091.
E-mail address: ndungup@ukzn.ac.za (P. Ndungu).
0360-3199/$ – see front matter Copyright © 2012, Hydrogen Energy Publications, LLC. Published by Elsevier Ltd. All rights reserved.
doi:10.1016/j.ijhydene.2012.03.050

replacement for current conventional fuels, as it has some advantages over pure hydrogen. These advantages include; liquid at room temperature, easier to integrate into current fuel infrastructure, good volumetric energy density, applicability in mobile power technologies, and highly efficient energy conversion [5,7–9].

The platinum catalyst is one of the most expensive components of a fuel cell, and as a result much R&D has been focused on reducing the platinum component in fuel cells; either by combining the catalyst with various metals (bi-, tri-metallic, or quaternary catalysts) or improving dispersion [3–9]. However the simplest way to minimize platinum usage is lower weight percent, and finer dispersion of the metal, alternatively processes that utilize fewer steps and less solvent during synthesis of the catalysts would more than likely allow for more cost saving benefits and lower the impact the synthesis of such materials would have on the environment. Such green chemical routes have been demonstrated using supercritical carbon dioxide, and water as the key solvent [4]. In contrast, solvent-less techniques; specifically, metal-organic chemical vapour deposition (OMCVD), have been used to prepare various catalysts [10,11] and electrocatalysts [12,13], and depending on the protocol developed, such methods can simplify the synthesis procedure, and reduce or eliminate the need for solvents.

In this paper we present a simple OMCVD method that can be used to synthesize highly dispersed Pt and PtRu nanoparticles and nanoclusters supported on carbon Nanomaterials. The procedure is a modified dry-mix method that produces particles with a very narrow size distribution, and results in stable nanoclusters with excellent electrochemical activities.

2. Experimental methods

The carbon supports used were either MWCNTs (Cheap Tubes Inc©, nominal outer diameter 20–30 nm, and length 20–30 μm) or Vulcan® XC–72 (Cabot Corporation™). The metal precursors, platinum (II) acetylacetonate (97%) and ruthenium (III) acetylacetonate (97%), were purchased from Sigma–Aldrich. Acids used for all pre-treatment steps were obtained from a local supplier (Kimix, South Africa).

2.1. Pre-treatment of the supports

The Vulcan® XC–72 (Cabot Corporation™) was pre-treated by first refluxing, under air, a known mass of the carbon with a 2.0 M HCl solution for 3 h, and then treating with 5.0 M HNO_3 solution at room temperature for 3 h. Finally the sample was washed with boiling distilled water until the pH of the rinsed solution reached 5.5. The treated sample was then dried at 110 °C, overnight. A typical run used 2.0 g of Vulcan® XC–72, 50.0 mL of HCl acid, and 50.0 mL of HNO_3.

MWCNTs were pre-treated using typical mixed acid systems; specifically, 1.0 g was refluxed with a 50.0 mL mixture of 98% H_2SO_4 and 55% HNO_3 (volume ratio of 2:3) for 1 h. The sample was then washed with distilled water until the pH of the rinsed solution reached 6–7. The treated sample was then dried in an 80 °C oven, overnight.

2.2. Deposition of metal clusters and nanoparticles

The method used was based on a modified dry-mix method using metal-organic chemical vapour deposition (OMCVD). A homemade stainless steel reactor, presented in Fig. 1, was designed and assembled using commercial parts (Swagelok®).

Using a mortar and pestle, a pre-weighed amount of platinum acetylacetonate [Pt (acac)2)] was thoroughly mixed with 500.0 mg of dry pre-treated carbon nanotubes or activated carbon. The sample was then transferred to the stainless steel reactor tube. The reactor tube was connected to a vacuum line, and then placed inside a ceramic work tube located inside a horizontally aligned tube furnace. The reactor was evacuated for 1 h, and the pressure was recorded (typical values were $\sim 7.7 \times 10^{-1}$ mbar) at room temperature. The tube furnace was then ramped to 100 °C (5 °C/min) and kept at 100 °C for another 1 h to remove surface condensates. During this step the pressure decreased to 2.8×10^{-1} mbar. The furnace was then ramped to 400 °C at a rate of 24 °C/min, and then held at the final temperature for 30 min to decompose the platinum precursor. The reactor tube was cooled to room temperature, and the sample was recovered. A similar procedure was used to deposit ruthenium on the pre-treated carbons or carbons with Pt deposits.

For comparative purposes, a wet chemical (WC) method was used to deposit the metals on the pre-treated supports. This is a polyol method based on our earlier work, and details can be found in reference [14]. In brief, 500 mg of the carbon support was mixed with 50 mL of ethylene glycol (EG) and treated with ultrasound in an ultrasonic bath for 20 min 8.45 mL of a 7.4 mg/mL chloroplatinic acid solution (EG solvent), was slowly added to the suspension, which was then stirred for 4 h. After stirring, the solution was titrated with 1M NaOH until pH = 8 and then kept at 130 °C, in an oil bath, for 3 h. Finally, the solution was left to cool to room temperature and then filtered. The product was dried under vacuum at 80 °C for 8 h. The nominal loading of Pt on the catalyst was 10%.

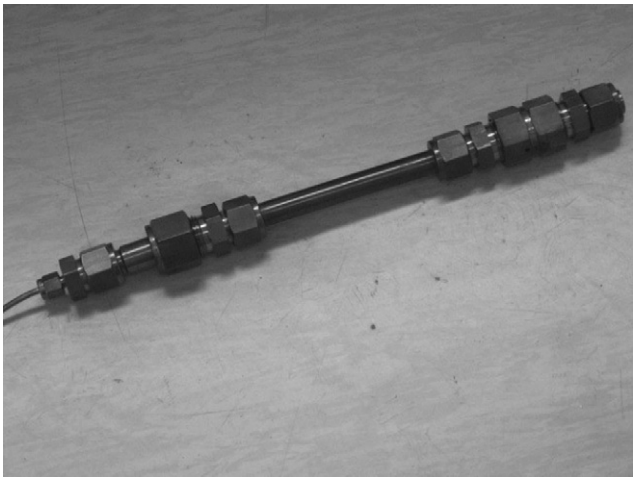

Fig. 1 – The assembled stainless steel reactor used for all OMCVD experiments; the main body sits within the furnace, whilst some of the evacuation line remains outside the furnace to prevent damage to the ball valve.

2.3. Characterization

Samples were characterized using X-ray diffraction (XRD) using a Siemens D8 Advance diffractometer with a Cu Kα radiation source operating at 40 kV; scanning electron microscopy (SEM) with energy dispersive X-ray spectroscopy (EDS) on a Hitachi X-650; ICP - MS using an Agilent 7500 CE ICP-MS with a High Matrix Introduction accessory and He as the collision gas; nitrogen sorption at 77 k on a Micrometrics ASAP 2020; and high resolution transmission electron microscopy (HRTEM) on a Tecnai G^2 electron microscope operating at 200 kV.

2.4. Electrochemical activity

The electrochemical (EC) activity and active surface area of the catalysts were evaluated by cyclic voltammetric (CV) using a BAS/50W integrated automated electrochemical workstation (Bioanalytical Systems, Lafayette, IN, USA). A conventional three electrode cell was used with an Ag/AgCl reference electrode, a platinum wire as the counter electrode and a homemade paste electrode as the working electrode.

The paste electrode was prepared by initially hand mixing ultra-pure graphite powder (Sigma–Aldrich) and mineral oil (Sigma–Aldrich) using a ratio of 70:30 (w/w) in an agate mortar and pestle. The resulting homogenous paste was then mixed with the catalyst of interest, using a 1:10 (w/w) ratio, and thoroughly mixed in an agate mortar and pestle. The catalyst paste was then tightly packed into a PVC tube (2 mm internal diameter) and a copper wire was inserted into one end of the tube to provide an electrical connection.

0.5 M H_2SO_4 was used as the initial electrolyte, which was then modified by the addition of methanol to obtain a final concentration of 0.5 M of methanol. The measured potential range was from −0.2 to 1.0 V (vs. Ag/AgCl) at a sweep rate of 50 mV/s. All CV cycles were done in a de-aerated solution (bubbled nitrogen gas through the solution for 30 min), and under a blanket of nitrogen.

The measured charge for hydrogen desorption Q_r was used to calculate the active platinum surface area of the electrodes and the following equation was used for the relevant calculations:

$$\mathrm{ESA} = \frac{Q_r}{m \times C} \quad (1)$$

Where Q_r (mC/cm^2) was measured from the area of the hydrogen absorption/desorption peak on the corresponding CV in the initial 0.5 M H_2SO_4 electrolyte, m (g) is the platinum loading confirmed from the ICP results, and C (0.21 mC/cm^2) is the charge of a monolayer of hydrogen absorbed/desorbed on a smooth platinum surface.

3. Results and discussion

Table 1 presents a summary of the various catalysts prepared, and a comparison of the theoretical loading versus the values obtained using EDS and ICP-MS.

At 10 wt% metal loading there is good agreement between the theoretical and measured values using both analytical techniques. It is interesting to note that the WC method seems to produce slightly smaller final loadings than the OMCVD method, on both supports used, and this can be attributed to incomplete reduction of the precursor during the WC method. Thus at the low loadings the OMCVD method not only simplifies the procedure needed to produce catalysts, but leads to less waste of the precious metal.

Table 1 – Comparison of EDS and ICP analysis on the benchmark catalyst, and the various samples prepared using WC and OMCVD methods.

Catalyst	Theoretical Metal content (wt%)	Metal content from EDS (wt%)	Metal content from ICP (wt%)	Synthesis Method
Pt/C	10	9.2	9.4	WC
Pt/CNT	10	9.5	9.3	WC
Pt/C	10	9.9	9.8	OMCVD
Pt/CNT	10	9.8	9.8	OMCVD
Pt/CNT	20	22	20	OMCVD
Pt/CNT	40	31	39	OMCVD
JM 40% Pt/CNT	40	39	42	N/A
Pt/CNT	60	50	59	OMCVD
PtRu/C (JM)	40:20	36:18	41:22	N/A
PtRu/CNT	20:20	17:15	19:20	OMCVD

Some deviations are observed with the samples prepared with 20, 40 & 60 wt% loading, in terms of theoretical versus actual loading, and between the two methods of analysis. EDS is a relatively quick and simple method for the characterization of carbon based catalysts, and with proper sample preparation and adequate data capture it can produce reliable results. However, some of the main limitations with EDS, versus analytical techniques such as ICP-OES, are the small sample size used for the analysis, inferior level of precision, and low detection limits [15]. As such, the deviations observed between the EDS measurements and ICP-OES results in Table 1 are mainly due to the aforementioned limitations with EDS analysis.

The small discrepancies between the theoretical and actual loadings can be ascribed to deposition of the metal on the side walls of the reactor, loss of precursor during the evacuation process, or excessive deposition of the vaporized material in cooler parts of the evacuation line. However, the method does produce material with values close to the desired loadings, despite the fact that the volume occupied by the catalyst support in the reactor is much smaller than the volume of the reactor itself. This also supports the view, as expected, that the precursor will deposit on the largest surface area available i.e. the catalyst support. Further room for improvement may be achieved with re-designing the reactor so as to minimize temperature gradients, or increasing the amount of support used per run.

3.1. X-ray diffraction

Typical XRD patterns on the samples prepared are presented in Fig. 2. Pt diffraction peaks were identified, using Joint Committee of Powder Diffraction Standards (JCPDS), at 39.8, 46.2, 68.1, 81.4 and 86.7° 2Θ; which corresponds to Pt (111),

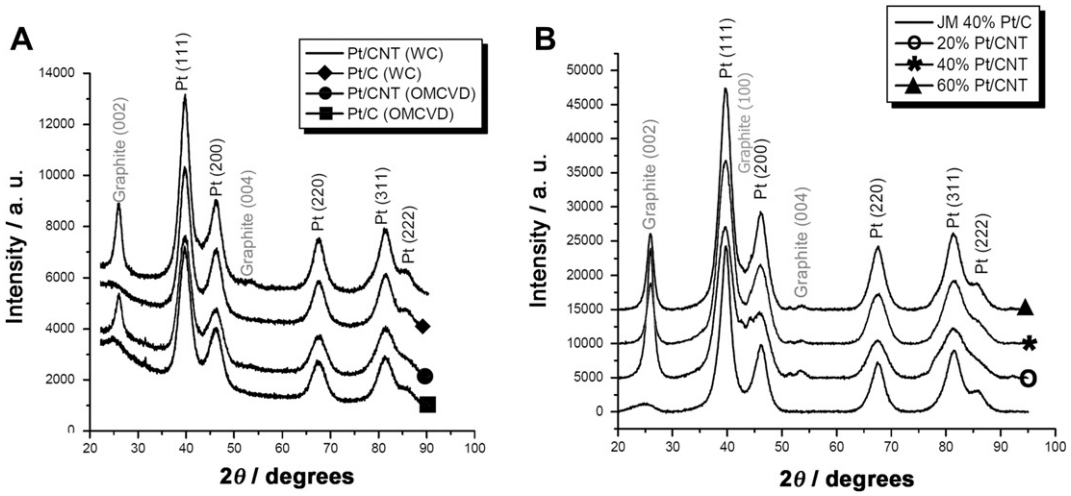

Fig. 2 – (A) XRD patterns of the 10 wt% samples synthesized using WC and OMCVD methods; (B) XRD patterns of the commercial benchmark catalysts, and the indicated samples synthesized using the OMCVD method.

(200), (220), (311) and (222) crystal faces, which are characteristic of fcc platinum. Furthermore, from these results it is clear that the catalysts made by CVD and WC methods, all have a Pt (fcc) crystal structure irrespective of the support used. A minor peak at 42.40° 2θ, was observed with the 20% Pt/CNT samples, and was attributed to the Graphite (100) reflection of carbon nanotubes.

All the CNT samples had the characteristic graphitic diffraction peak at a 2θ value of ~26°. The same peak was broad and had a very low intensity in the case of the activated carbon samples and JM benchmark sample. This difference is due to the highly ordered helical arrangement of the graphene sheets in the CNTs and layered and almost random structuring of the activated carbon supports, and as such the CNTs are crystalline and the activated carbons are amorphous in nature. These observations are in line with what has been reported in the literature [16].

The XRD pattern for the PtRu/CNT sample synthesized using the OMCVD technique is presented in Fig. 3, along with the commercial sample. For the Pt/CNT (40 wt%) sample, the Pt peaks occur at 2θ values of 39.0° and 67.5° for Pt (111) and Pt (220). With the PtRu samples, these peaks are displaced to 41.0° and 69.0° respectively, which is indicative of PtRu alloy formation [3,17]. In addition to the alloy peaks, there are separate Ru peaks on the PtRu/CNT sample at 2θ values of 43.5° and 78.5°, which are ascribed to Ru (101) and Ru (103) of hcp Ru. The broadening of the peaks on the PtRu/CNT samples is due to the small particle size of the metal deposits [3,17].

The average particle size of the metal deposits was determined using the Scherrer equation.

$$d = \frac{k\lambda}{\beta_{1/2}\cos\theta} \quad (2)$$

Table 2 summarizes the calculated values for the average particle size on the various samples using the Scherrer equation. It can be seen that the angle of diffraction (2θ value) for Pt catalysts are similar, which is between 39.4 and 39.9 2θ degree. The reason for this small shift is unclear at this time; however, it can either be due to instrument error, nanoparticle strain [18], or slight amount of impurities with the WC samples [17]. Meanwhile for the Pt-Ru alloy there is an increase in 2θ value due to the incorporation of the relatively smaller Ru atom into the fcc structure of Pt [19]. From the tabulated data it is clear that the WC method produced particles with a larger average size, and the OMCVD method produces smaller particles when compared to the benchmark sample, even at much higher loadings. As expected, the PtRu/CNT samples had relatively small particle sizes in the low nanometer range, and correlates well with the broadening observed in the XRD pattern (Fig. 3).

3.2. *TEM investigations*

Typical TEM images, and corresponding particle size histograms (200 count per image), on the 10 wt% samples are

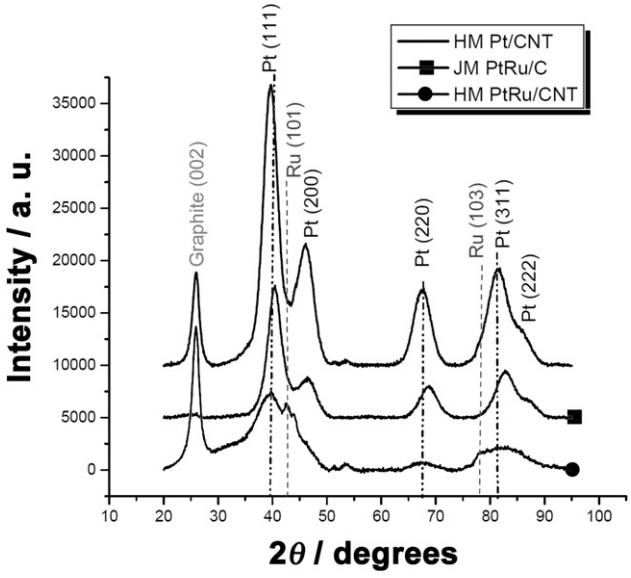

Fig. 3 – XRD patterns of the homemade PtRu/CNT sample, Pt/CNT sample, and a commercial sample of PtRu/C.

Table 2 – Summary of key parameters obtained from XRD, TEM, and CV analysis on the samples synthesized using WC and OMCVD methods.

Sample	Pt (111) (2θ, degree)	[Pt] (mg/cm^2)	Qr (μC)	ECSA (m^2/g-Pt)	Particle size by TEM (nm)	Particle size from XRD (nm)
10 wt.% Pt/C-WC	39.5	0.00094	18	91	2.89	2.65
10 wt% Pt/CNT-WC	39.5	0.00093	21	107	2.94	2.78
10 wt% Pt/C-OMCVD	39.4	0.00098	26	138	2.31	2.12
10 wt% Pt/CNT-OMCVD	39.4	0.00098	30	153	2.50	2.42
JM 40% Pt/C	39.9	0.0042	168	190	3.28	3.76
20 wt% Pt/CNT	39.6	0.0017	61	170	2.61	2.72
40 wt% Pt/CNT	39.8	0.0036	152	201	2.77	2.89
60 wt% Pt/CNT	39.9	0.0055	175	151	3.22	3.43
JM PtRu/C	41.0	0.0058	194	159	2.01	1.88
40PtRu/CNT	41.0	0.0035	158	215	1.75	1.57

presented in Fig. 4. The samples prepared using the WC method had relatively more agglomerates than the samples prepared using the OMCVD technique and the size distribution of the metal was much narrower with the OMCVD method.

Using the WC method, the average particle size of the Pt/C and Pt/CNT samples were 2.89 and 2.94 nm respectively, whereas the OMCVD method produced average sizes of 2.31 and 2.50 nm on Pt/C and Pt/CNT respectively. Despite the use of relatively high temperatures in the OMCVD process, the method produces lower levels of agglomeration, and nanoparticles with a smaller average diameter than the WC method.

Fast nucleation rates favour formation of small NP's. On CNTs, a heterogeneous nucleation mechanism has been proposed, which can be optimized through the use of surfactants to produce small NP's on the surface of CNTs [20]. In OMCVD processes nucleation rate increases with temperature [10–13], & the lack of competing solvent molecules favours higher nucleation rates, hence the better dispersion on CNTs. Further work that looks at differences in surface chemistry & energy (use of annealed CNTs, doped CNTs and CNTs precoated with oxides or metals) and how it affects particle size distribution are on-going. However some tentative comments are made below with the PtRu/CNT samples.

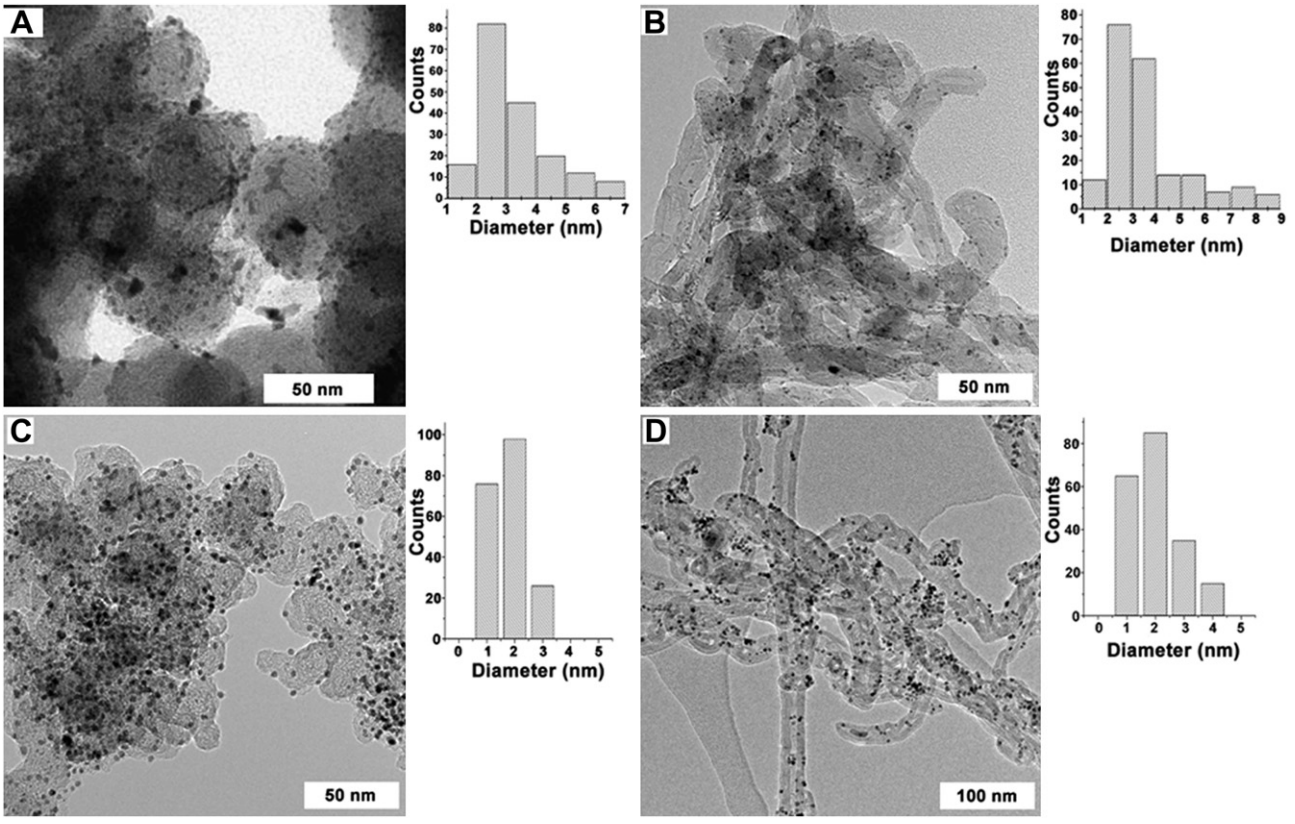

Fig. 4 – TEM images on (A) Pt on AC synthesized using WC method; (B) Pt on CNT using the WC method; (C) Pt on AC using OMCVD method; and (D) Pt on CNT using OMCVD method. All samples are in the figure are 10 wt% metal on support.

Samples prepared with larger loadings had a similar profile to the 10 wt% samples; specifically, narrow particle size distribution, very little agglomeration, and excellent dispersion. The exception was the extremely high loading sample of 60 wt% (Fig. 5).

From the particle size count, obtained from the TEM images, the average Pt particle sizes were 2.61, 2.77 and 3.82 nm for the 20, 40 and 60 wt% loadings. It is interesting to note that the histograms for the 10–40 wt% samples were similar, with a narrow distribution of sizes between 0.5 and 4.5 nm, and the 60 wt% Pt/CNT sample had slightly increased range from 0.5 to 6.5 nm. All the samples were prepared using the same OMCVD parameters, thus nucleation and growth rates were similar, and can explain the histogram profiles for the 10–40 wt% samples, and the significant count of nanoparticles with a size of 0.5 nm for the 60 wt% sample. Thus the OMCVD parameters used resulted in a high nucleation rate and density, and the increased size range obtained with the high loading sample can be attributed to the increased amount of material, allowing for coalescence phenomena to occur on the surface of the material, similar results have been reported elsewhere [12,13].

From the TEM images and particle size analysis (200 count), the PtRu/CNT samples had an average particle size of 1.75 nm and the histogram values ranged from 0.5 to 3.5 (Fig. 6). Ruthenium acetylacetonate has been reported to start decomposing at 285 °C in an inert atmosphere, and in low pressure systems for film growth, Ru thin films have been produced using substrate temperatures between 300 and 370 °C [21]. In contrast, platinum acetylacetonate has been reported to decompose at temperatures as low as 155 °C, with complete decomposition at 255 °C [22].

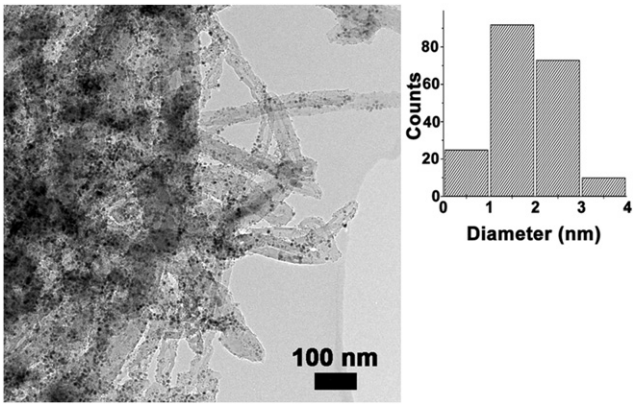

Fig. 6 – TEM image of the 20:20 wt% PtRu/CNT sample, with corresponding particle size distribution.

Thus it is highly likely the Pt nanoparticles nucleate and grow first, followed by the ruthenium nanoparticles, and from the XRD results, it would seem that the Ru deposits on the Pt and any Pt free sites on the supports. Co-deposition is very unlikely due to the stability of the Ru precursor in the vapour phase.

It should be noted that the literature has several examples of WC methods that have produced finely dispersed Pt

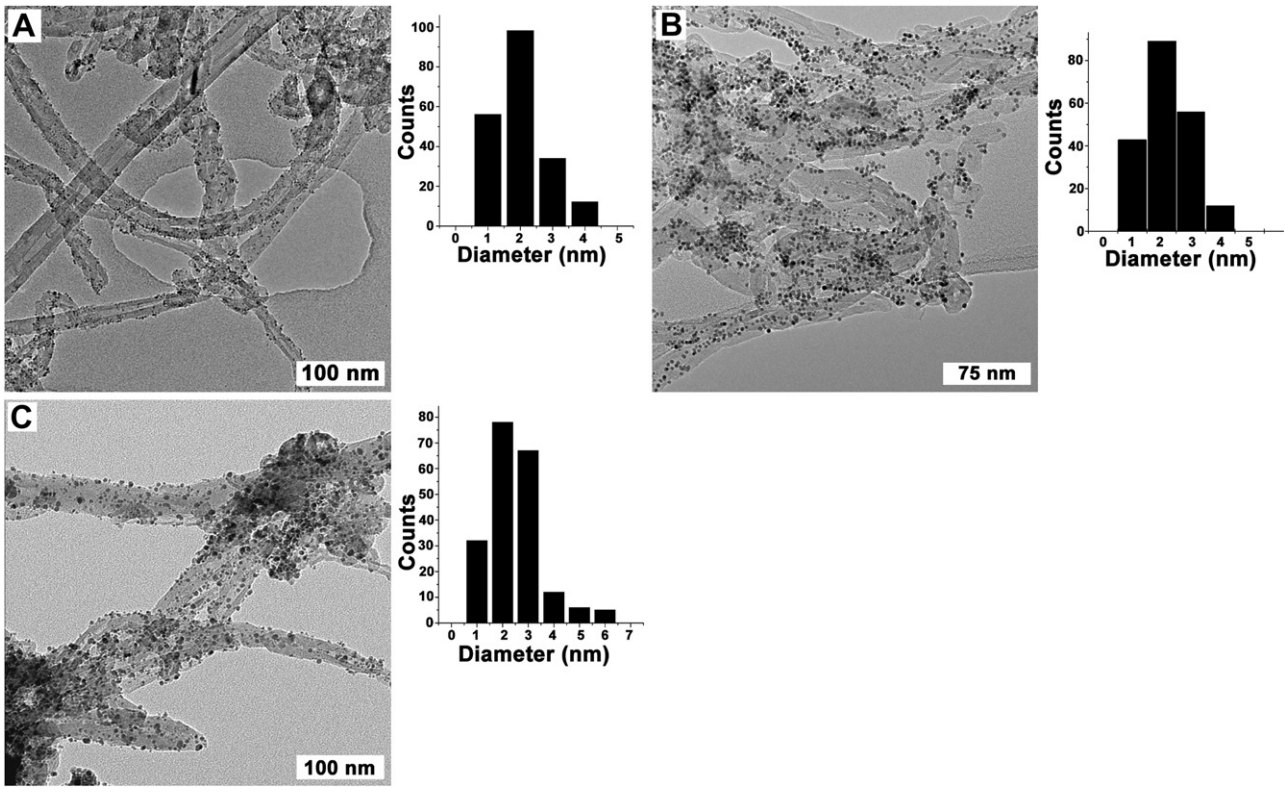

Fig. 5 – TEM images of 20 wt% and corresponding size histogram (A); 40 wt% and corresponding size histogram (B); 60 wt% and corresponding size histogram (C) of Pt nanoparticles on CNT supports.

nanoparticles on carbon nanotubes supports (for some examples see refs [4,5,7,9]), and although our CVD method, compared to our WC method, results in a system with superior characteristics, its main advantage is the elimination of solvents, and the use of fewer steps.

3.3. HRTEM

Further studies on the OMCVD samples using HRTEM, revealed some interesting features unique to the CNT samples. In Fig. 7(A), the STEM image of the PtRu nanoparticles on the CNT shows small particles, and bright lines that are next to the metal nanoparticles.

These features are not present in the samples prepared on activated carbon (Fig. 7(B)), or on samples prepared using WC methods. The lack of these features on the activated carbon can be explained by the difference in structure between the CNT and activated carbon; specifically, the ordered layers of graphene sheets with the CNT. During the OMCVD process metal precursor decomposes to metal atoms, which may then pass through defect sites and enter the layers between the graphene sheets. However, the activated carbon samples did have isolated metal clusters close to the nanoparticles (Fig. 7(B)), which supports the view that the precursor decomposes to form isolated clusters that can diffuse through defects present. The role these clusters may play in electrochemical activity is commented on in the next section.

3.4. Electrochemical activity

Typical cyclic voltammograms (CV) on the various 10 wt% samples are presented in Fig. 8. The Hydrogen desorption peak was observed within the potential range of −0.21 to 0.10 V and the Oxygen reduction peak between 0.30 and 0.80 V.

The peaks demonstrate that all of the 10 wt% catalysts are active for hydrogen and oxygen redox processes, and the least active catalysts are the ones prepared using the WC method. This trend was confirmed with the calculated values of the electrochemically active surface area (ECSA), presented in Table 2.

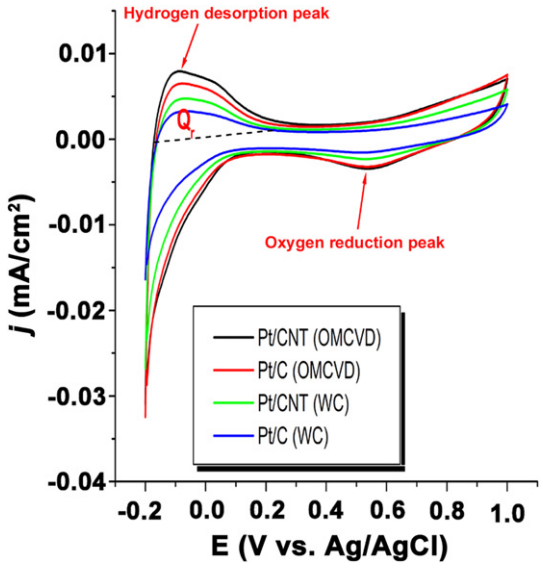

Fig. 8 – Cyclic voltammograms on the 10 wt% samples in a nitrogen degassed solution of 0.5 M sulphuric acid, using a scan rate of 50 mV/s, and an Ag/AgCl reference electrode.

Heat treatment procedures on Pt/C catalysts, synthesized using various WC methods, have been shown to improve electrocatalytic activity, due to removal of surface impurities, or improved dispersion and stability of the metal [23]. In terms of the ECSA, there is a 52% (comparing Pt/C) and 43% (comparing Pt/CNT) increase when changing from a WC to OMCVD process. The much greater activity with the OMCVD catalysts can be attributed to the smaller particle size, narrow size distribution, and the much cleaner surface of the NP's, due to lack of solvent, surfactants, and other potential interfering species. But the transition from an activated carbon support to a CNT support, shows a further enhancement of ~ 11%, despite the Pt/C–OMCVD catalysts having a smaller particle size as determined by TEM and XRD. Recently, it was reported that smaller Pt nanoparticles are intrinsically more active as electrocatalysts [24,25]. Our current results support

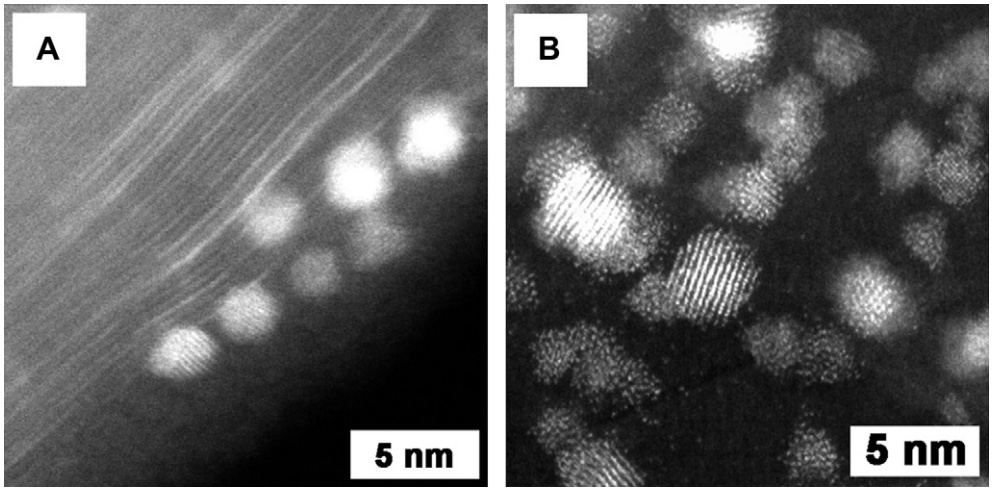

Fig. 7 – A) CNT with PtRu NP'S on the surface and metal atoms between CNT walls, as represented by bright lines; B) PtRu nanoparticles on activated carbon support highlighting the absence of bright line features seen with the CNT.

these earlier presentations (comparison between WC and OMCVD synthesized samples), and the additional enhancement observed with the CNT-OMCVD catalysts is an expected result, due to the excellent physical-chemical properties of CNT. Recently, Shao-Horn et al clearly demonstrated a direct correlation between the amount of under-coordinated Pt atoms, typical of nanoparticles below 3 nm, and the electrocatalytic activity of Pt/CNT catalysts [25]. Thus the role of the Pt clusters/atoms that are stabilized by the defect sites on the CNTs (on Pt/CNT-OMCVD samples in Fig. 7) can have a similar role and merits further investigation.

The CV's of the various 10 wt% samples in an acidic methanol solution are presented in Fig. 9. For all catalysts the oxidation of methanol is observed in the forward anodic scan at ~ 0.7 V (A), and the reverse scan shows an oxidation peak, at ~ 0.5 V (B), which are typical features seen with these types of curves [3–9,17,21].

Summary of the key data from the CV's in Fig. 9 are presented in Table 3. With the WC samples, the peak current density for the methanol oxidation peak in the forward scan was highest with the Pt/CNT-WC sample, and similarly with the OMCVD samples the Pt/CNT-OMCVD sample had the highest peak current density.

From the table, it is clear that the samples follow the expected trend determined by the ECSA values. CNT supported samples make superior electrocatalysts, and the catalysts synthesized using the OMCVD process are kinetically superior, and hence have much higher peak currents than the corresponding WC samples. These results emphasize the synergy inherent to NP's – support systems in electro-catalysis.

3.4.1. *Higher loading samples*

The 20–60 wt% samples and the commercial sample were observed to have similar CV to the 10 wt% samples, when measured in the 0.5 M sulphuric acid solution (Fig. 10).

From the calculated ECSA values (Table 2), the 40 wt% Pt/CNT catalyst had superior electrocatalytic characteristics when compared to the commercial Johnson Mathey catalyst, and is due to the narrow size distribution, smaller particle size, and lack of interfering surface species on the homemade OMCVD catalyst. The drop with the 60 wt% sample is due to agglomeration and larger average particle size.

The CV's for the samples in the acidic methanol solution are presented in Fig. 11, and show that the 40 wt% sample outperformed the commercial sample.

This is clearly illustrated in the peak currents, and peak current ratios; however, the onset potentials are very similar with a less than 10% variation in the values (Table 3). The onset potential has been used as an indication of the electron transfer kinetics for methanol oxidation, with lower values

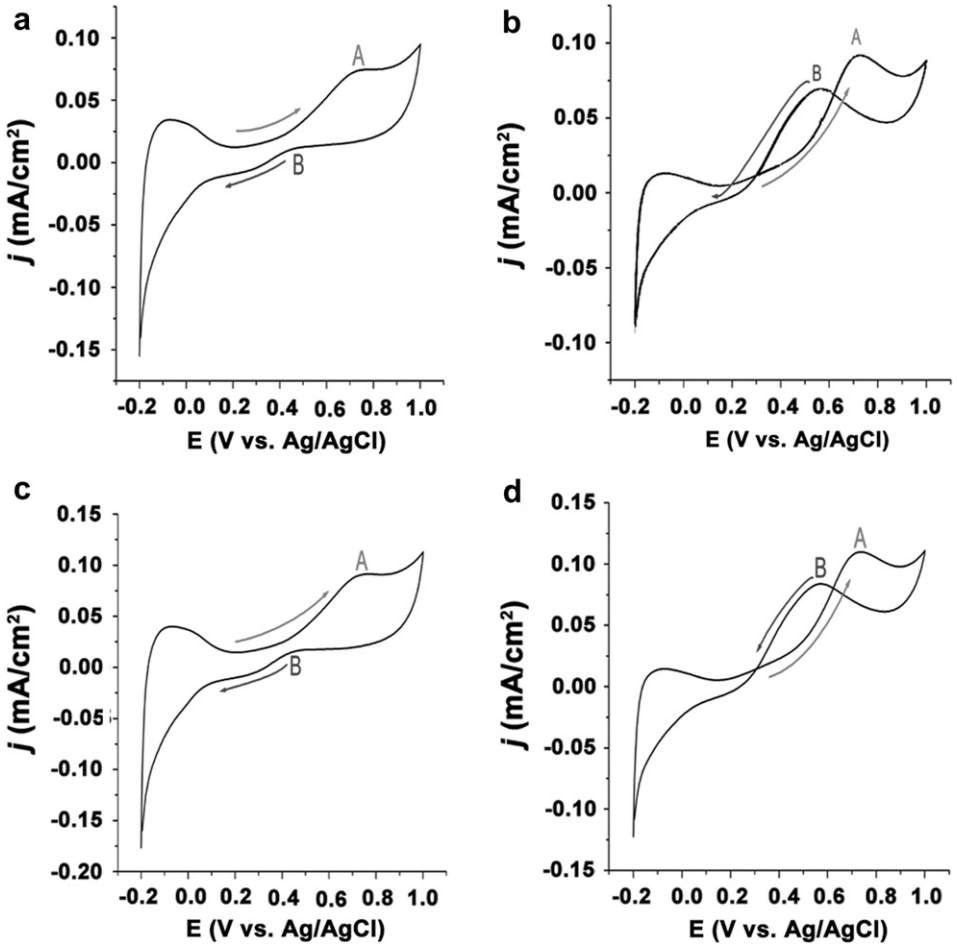

Fig. 9 – CV of 10 wt% samples in a 1.0M sulphuric acid + 0.5 M methanol solution, de-aerated with nitrogen; (a) Pt/C using WC methods, (b) Pt/CNT using WC methods, (c) Pt/C using OMCVD methods, and (d) Pt/CNT using OMCVD methods.

Table 3 – Peak potential and peak current ratios for the 10 wt% catalysts and the higher loading samples taken in a 0.5 M H_2SO_4 + 0.5 M CH_3OH solution.

Catalyst	Onset potential (V)	Peak potential (V)	Peak current I_f (A) (mA/cm^2)	I_r (B) (mA/cm^2)	I_f/I_r
10 wt% Pt/C-WC	0.269	0.742	70	19	3.68
10 wt% Pt/CNT-WC	0.264	0.733	99	68	1.46
10 wt% Pt/C-OMCVD	0.269	0.742	82	20	4.10
10 wt% Pt/CNT-OMCVD	0.269	0.772	115	78	1.47
JM 40% Pt/C	0.303	0.721	182	122	1.49
20 wt% Pt/CNT	0.283	0.724	149	103	1.45
40 wt% Pt/CNT	0.313	0.703	200	140	1.43
60 wt% Pt/CNT	0.283	0.761	137	103	1.33
JM PtRu/C	0.283	0.782	140	105	1.33
40 PtRu/CNT	0.303	0.720	205	148	1.39

indicative of an improvement over benchmark catalysts [3,22]. The small variation seen between the samples suggests that the enhanced electrochemical activity observed with the homemade catalysts is not necessarily due to improved kinetics, and maybe due to the prevalence of small metal nanoparticles and clusters as discussed above.

The I_A/I_B ratio has been used to determine the tolerance of such catalysts to CO, with larger values regarded as a positive sign the material synthesized is an excellent CO resistant catalyst [3,22]. The ratio's reported may seem to contradict this assumption, since there are numerous examples in the literature that have shown PtRu catalysts are the best system for DMFCs [3,4,6,8,22]. What the values are showing, is that in our testing system, this cannot be used as such an indicator, and can be attributed to the complex mechanism associated with methanol oxidation, where it has been suggested that the oxidation of methanol can occur over the wide potential window used for characterizing the catalysts [22,26]. Thus the clearest indication that the homemade catalysts are indeed superior in performance characteristics when compared to the benchmark JC catalysts, is the fact the forward and reverse peak currents are the largest for the 40 wt% Pt/CNT when compared with JM 40 wt% Pt/C, and for the 40 wt% PtRu/CNT versus the JM PtRu/C.

Recently, Wang et al demonstrated that PtRu/C catalyst activity for methanol oxidation can be enhanced by heat treatments in hydrogen, and more notably, nitrogen

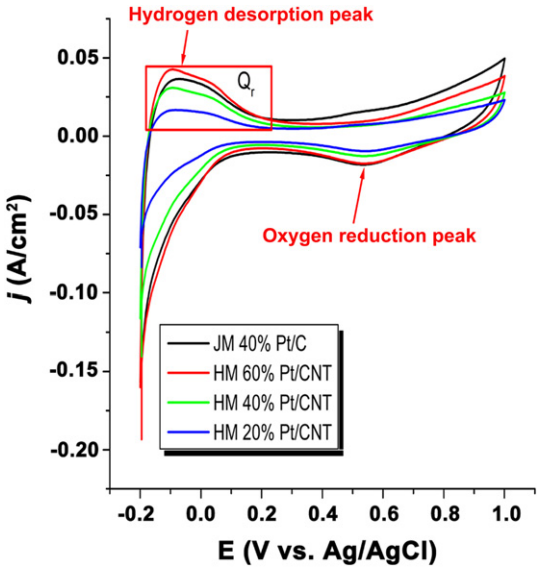

Fig. 10 – Cyclic voltammograms of Pt/CNT and JM Pt/C electrocatalysts.

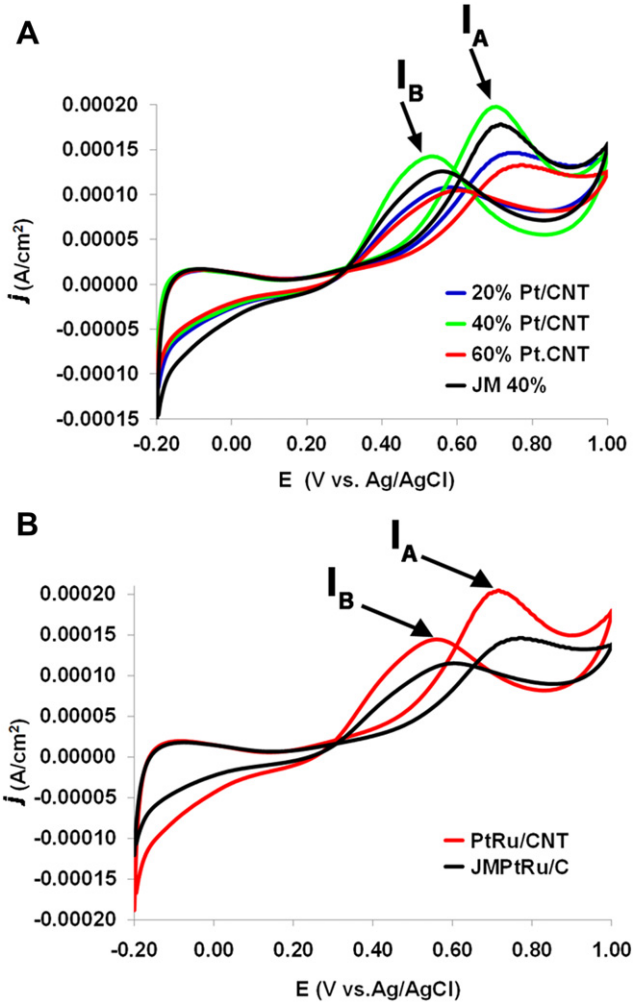

Fig. 11 – CV on commercial and various homemade supported catalysts in a 0.5 M H_2SO_4 + 0.5 M methanol solution. Panel (A) consists of the samples with Pt only, and panel (B) are the PtRu samples.

atmospheres, due to some segregation of the PtRu particles after 1 h at 570 K[27]. The OMCVD synthesis method resulted in some separate Ru phase (see Fig. 3), and thus the enhanced catalytic activity can also be due to a similar reason i.e. some separate Pt and Ru phases having a synergistic effect (keeping in mind the small particle size, excellent dispersion, and stabilised clusters on the CNT) on the electro-catalysis.

It should be noted that further studies are underway to determine if this method can produce different atomic ratios of Pt: Ru supported on CNTs to further enhance the positive results seen so far.

4. Conclusions

A relatively simple solvent free technique has been successfully applied to produce Pt and Pt-Ru nanoparticles supported on CNT as highly active DMFC catalysts. The Metal-organic chemical vapour deposition technique used resulted in well dispersed nanoparticles with a very narrow size distribution. The OMCVD method developed produced unique metal clusters/atoms distributed between the graphene sheets of the CNT, and stabilized by the CNT defects. The platinum nanoparticles produced using a WC or OMCVD method, resulted in fcc crystal structures on all supports used, and the smallest average nanoparticles were observed on OMCVD samples.

The electrochemical activity of the catalysts were tested using CV, and the initial work comparing the WC and OMCVD catalysts found the OMCVD samples supported on CNTs to have the highest activity. Subsequent tests on high loading samples, 20–60 wt% Pt/CNT showed that the 40 wt% sample had greater electrochemical activity that the JM commercial catalyst. The PtRu/CNT catalyst showed similar improvements over the JM PtRu/C commercial catalyst.

The interesting results from the OMCVD catalyst are being explored further in membrane electrode assemblies, and further work into synthesizing more complex metal systems such as tri-metallic systems are underway. We anticipate such work will allow for new effective and quick synthetic strategies for catalysts systems for fuel cells.

Acknowledgements

The authors would like to thank Neil Young from the University of Oxford for discussions and assistance with the HRTEM work, Basil Juiles and Adrian Josephs from the University of the Western Cape for their assistance with TEM analysis, and Remy Bucher (iThemba LABS) for XRD measurements.

REFERENCES

[1] Serov A, Kwak C. Review of non-platinum anode catalysts for DMFC and PEMFC application. Appl Catal B 2009;90:313–20.
[2] Jaouen F, Herranz J, Lefevre M, Dodelet J-P, Kramm UI, Herrmann I, et al. Cross-laboratory experimental study of non-noble-metal electrocatalysts for the oxygen reduction reaction. ACS Appl Mater Interfaces 2009;1:1623–39.
[3] Xu M-W, Su Z, Weng Z-W, Wang Z-C, Dong B. An approach for synthesizing PtRu/MWCNT nanocomposite for methanol electro-oxidation. Mater Chem Phys 2010;124: 785–90.
[4] Shimizu K, Wang JS, Wai CM. Application of green chemistry techniques to prepare electrocatalysts for direct methanol fuel cells. J Phys Chem A 2010;114:3956–61.
[5] Chen Y, Zhang G, Ma J, Zhou Y, Tang Y, Lu T. Electro-oxidation of methanol at the different carbon materials supported Pt nano-particles. Int J Hydrogen Energy 2010;35: 10109–17.
[6] Chang W-C, Nguyen MT. Investigations of a platinum–ruthenium carbon nanotube catalyst formed by a two-step spontaneous deposition method. J Power Sources 2011;196:5811–6.
[7] Salgado JRC, Duarte RG, Ilharco LM, Botelho do Rego AM, Ferraria AM, Ferreira MGS. Effect of functionalized carbon as Pt electrocatalyst support on the methanol oxidation reaction. Appl Catal B 2011;102:496–504.
[8] Hsu N-Y, Chien C-C, Jeng K- T. Characterization and enhancement of carbon nanotube-supported PtRu electrocatalyst for direct methanol fuel cell applications. Appl Catal B 2008;84:196–203.
[9] Li W, Liang C, Zhou W, Qiu J, Zhou Z, Sun G, et al. Preparation and characterization of multiwalled carbon nanotube-supported platinum for cathode catalysts of direct methanol fuel cells. J Phys Chem B 2003;107:6292–9.
[10] Serp P, Kalck P, Feurer R. Chemical vapor deposition methods for the controlled preparation of supported catalytic materials. Chem Rev 2002;102:3085–128.
[11] Thurier C, Doppelt P. Platinum OMCVD processes and precursor chemistry. Coord Chem Rev 2008;252:155–69.
[12] Billy E, Maillard F, Morin A, Guetaz L, Emieux F, Thurier C, et al. Impact of ultra-low Pt loadings on the performance of anode/cathode in a proton-exchange membrane fuel cell. J Power Sources 2010;195:2737–46.
[13] Garcia-Contreras MA, Fernandez-Valverde SM, Vargas-Garcia JR. Pt, PtNi and PtCoNi film electrocatalysts prepared by chemical vapor deposition for the oxygen reduction reaction in 0.5 M KOH. J Alloys Compd 2010;504: S425–8.
[14] Naidoo S, Naidoo QY, Vaivars G. Low temperature quaternary catalyst synthesis used for methanol and hydrogen oxidation on MWCNT. Integr Ferroelectr 2008;103: 80–9.
[15] Scaccia S, Goszczynsk B. Sequential determination of platinum, ruthenium, and molybdenum in carbon-supported Pt, PtRu, and PtMo catalysts by atomic absorption spectrometry. Talanta 2004;63:791–6.
[16] Narkiewicz U, Podsiadły M, Jedrzejewski R, Pełech I. Catalytic decomposition of hydrocarbons on cobalt, nickel and iron catalysts to obtain carbon nanomaterials. Appl Catal A 2010; 384:27–35.
[17] Gu Y-J, Wong W-T. Nanostructure PtRu/MWNTs as anode catalysts prepared in a vacuum for direct methanol oxidation. Langmuir 2006;22:11447–52.
[18] Ingham B, Hendy SC, Fong DD, Fuoss PH, Eastman JA, Lassesson A, et al. Synchrotron X-ray diffraction measurements of strain in metallic nanoparticles with oxide shells. J Phys D Appl Phys 2010;43. 075301 (6pp).
[19] Lizcano-Valbuena WH, Paganin VA, Gonzalez ER. Methanol electro-oxidation on gas diffusion electrodes prepared with Pt-Ru/C catalysts. Electrochim Acta 2002;47:3715–22.
[20] Wang Yu, Xu Xin, Tian Zhongqun, Zong Ye, Cheng Huiming, Lin Changjian. Selective heterogeneous nucleation and growth of size-controlled metal nanoparticles on carbon nanotubes in solution. Chem Eur J 2006;12:2542–9.
[21] Igor K, Igumenov PP, Semyannikov SV, Trubin NB, Morozova NV, Gelfond AV, et al. Approach to control

deposition of ultra thin films from metal organic precursors: Ru deposition. Surf Coat Technol 2007;201:9003–8.
[22] Utriainen M, Kroger-Laukkanen M, Johansson L-S, Niinisto L. Studies of metallic thin film growth in an atomic layer epitaxy reactor using $M(acac)_2$ (M = Ni, Cu, Pt) precursors. Appl Surf Sci 2000;157:151–8.
[23] Bezerra CWB, Zhang L, Liu H, Lee K, Marques ALB, Marques EP, et al. A review of heat-treatment effects on activity and stability of PEM fuel cell catalysts for oxygen reduction reaction. J Power Sources 2007;173: 891–908.
[24] Kim Y-T, Ohshima K, Higashimine K, Uruga T, Takata M, Suematsu H, et al. Fine size control of platinum on carbon nanotubes: from single atoms to clusters. Angew Chem Int Ed 2006;45:407–11.
[25] Lee SW, Chen S, Sheng W, Yabuuchi N, Kim Y-T, Mitani T, et al. Roles of surface steps on pt nanoparticles in electro-oxidation of carbon monoxide and methanol. J Am Chem Soc 2009;131:15669–77.
[26] Díaz V, Ohanian M, Zinola CF. Kinetics of methanol electrooxidation on Pt/C and PtRu/C catalysts. Int J Hydrogen Energy 2010;35:10539–46.
[27] Wei Y-C, Liu C-W, Chang W-J, Wang K-W. Promotion of Pt–Ru/C catalysts driven by heat treated induced surface segregation for methanol oxidation reaction. J Alloys Compd 2011;509:535–41.